JOURNAL OF COMPUTATIONAL PHYSICS 56, 1–14 (1984)

# Elimination of Spurious Modes in Finite Element Analysis

JOAB R. WINKLER AND J. BRIAN DAVIES

*Department of Electronic and Electrical Engineering, University College, London WC1E 7JE, England*

Received July 14, 1983; revised November 29, 1983

A common cause of spurious (non-physical) modes that arise in either finite difference or finite element derived eigenvalue problems is identified. It is shown that these modes are the result of an excessively flexible system. The flexibility is removed by constraining the problem. An analogy is drawn between electromagnetic wave propagation and acoustic wave propagation in liquids to show that the spurious modes encountered in both cases are due to fundamentally the same cause. Results are presented to show that constraining the problem yields a significant reduction in the number of spurious modes, a big improvement in the quality of the eigenvector of the physical modes and only a marginal increase in the error in the eigenvalue for the low order modes.

## I. INTRODUCTION

The finite element method [1] has enjoyed popularity in the last few years due to its success in solving field problems. However, one serious disadvantage of the method is the appearance of spurious modes in eigenvalue problems. A few authors [2–6] have referred to them but no satisfactory explanation has yet been offered for their existence, nor has a method yet been devised for their elimination. Konrad [2] suggests that spurious modes are caused by not forcing boundary conditions rigorously, but when tested computationally by Davies, Fernandez and Philippou [3] no significant reduction in the number of spurious modes occurred. In this paper another explanation for these spurious modes is offered and the results are considerably more successful.

## II. THEORY

Commonly used variational expressions for use in acoustics and electromagnetic problems are

$$\omega^2 = \frac{\int_\Omega (\mathbf{Av})^T \mathbf{c}(\mathbf{Av})\, d\Omega - \int_S \mathbf{v}^T \cdot [\mathbf{cAv}] \cdot d\hat{\mathbf{s}}}{\int_\Omega \mathbf{v}^T \rho \mathbf{v}\, d\Omega} \tag{1}$$



0021-9991/84 $3.00

and

$$\omega^2 = \frac{\int_\Omega (\nabla \times \mathbf{H})^* \, \|\varepsilon^{-1}\| \, (\nabla \times \mathbf{H}) \, d\Omega}{\int_\Omega \mathbf{H}^* \mu \mathbf{H} \, d\Omega} \tag{2}$$

respectively. The first is defined and developed in Section III. The second occurs in various references [2, 3, 18]. Other formulations can be used but there are good reasons for choosing (1) or (2) over alternatives. The contention of this paper is that on occasions, and in particular when using the above expressions, there is a lack of uniqueness in the vector field (**v** or **H**) of the corresponding Euler equations and so when used to formulate the finite element method, this can inevitably lead to an ill-conditioned system with resulting spurious modes.

A. *An Analogy Between Electromagnetic Wave Propagation and Acoustic Wave Propagation in Liquids*

Consider Maxwell's equations in a source free and uniform isotropic medium:

$$\nabla \times \mathbf{E} = -\partial \mathbf{B}/\partial t \tag{3a}$$

$$\nabla \times \mathbf{H} = \partial \mathbf{D}/\partial t \tag{3b}$$

$$\varepsilon \nabla \cdot \mathbf{E} = 0 \tag{4a}$$

$$\mu \nabla \cdot \mathbf{H} = 0 \tag{4b}$$

where each symbol has its usual meaning. Equation (3b) can also be written as

$$\nabla \times \{\mathbf{H} + \nabla \phi\} = \partial \mathbf{D}/\partial t \tag{5}$$

for all scalar fields $\phi$. This is an example of Helmholtz's theorem, that a vector field is only fully defined when both the divergence and the curl of the vector field are defined at every point in space. Hence a value must be assigned to $\nabla \cdot \mathbf{H}$ and (4b) states that this value is zero. Similarly, (4a) removes ambiguity in the vector **E** defined in (3a).

Next, consider the equation for wave propagation in compressible liquids. From Auld [7] the governing equation is

$$c_{11} \nabla [\nabla \cdot \mathbf{v}] = \rho \frac{\partial^2 \mathbf{v}}{\partial t^2} \tag{6}$$

where $c_{11}$ is the Lamé constant of the liquid, $\rho$ is its density and **v** is the velocity vector. Equation (6) can alternatively be written as

$$c_{11} \nabla \{\nabla \cdot [\mathbf{v} + \nabla \times \psi]\} = \rho \frac{\partial^2 \mathbf{v}}{\partial t^2} \tag{7}$$

for all vector fields $\psi$. This is another example of Helmholtz's theorem but this time the ambiguity is removed by placing a value on $\nabla \times \mathbf{v}$ at every point in space. Since liquids cannot support waves in which there is rotation, it follows that $\nabla \times \mathbf{v} = 0$ everywhere.

This analysis has shown there is a common problem of field representation for electromagnetic wave propagation and acoustic wave propagation in liquids. It is suggested that the ambiguity in the problem statement referred to above is one of the primary causes of spurious modes.

B. *The Finite Element Method and Constrained Optimisation*

In the finite element method [1] we seek a function $u$ that will minimise a functional (usually an energy functional) $J(u)$. The function $u$ is obtained by patching together element basis functions to form the global approximation. This is a problem in unconstrained optimisation. If, however, a constraint as discussed in Section IIA is imposed on the problem, then it becomes one of constrained optimisation, and three methods that are used to solve such problems are now considered. We may:

(1) Restrict the trial (basis) functions to lie in the admissible set of functions that actually satisfy the constraint.

(2) Modify the functional by the Lagrange multiplier method. The solution is now sought over all admissible functions.

(3) Modify the functional by adding a penalty term. As in (2) above, the solution is now sought over all admissible functions but by increasing the penalty parameter $\alpha$, the solution is forced to lie in an increasingly constrained set of admissible functions.

In method (1), the constraint is imposed a priori on the trial functions and no modification need be made to be functional. We have not used this method because it requires the construction of special basis functions and elements.

In method (2), a modified functional $J^*$ is constructed

$$J^*(\mathbf{x}, \mu) = J(\mathbf{x}) + \int_{\Omega} \mu g(\mathbf{x})\, d\Omega \tag{8}$$

where $\mathbf{x}$ denotes the set of element "nodal values," and the required constraint $g(x) = 0$ is imposed in the volume $\Omega$ by the Lagrange multiplier $\mu$. This method suffers from disadvantages, perhaps the chief one being that the system stiffness matrix now possesses zeros along the main diagonal. This can lead to computational difficulties because the matrix is now ill-conditioned. The technique was used with only partial success by Mabaya, Lagasse and Vandenbulcke [5] in the finite element analysis of optical waveguides. They found that specific enforcement of the natural boundary condition by the Lagrange multiplier method reduced the number of spurious modes, but did not eliminate them.

In method (3), the penalty function approach, the functional is augmented

$$J^*(\mathbf{x}) = J(\mathbf{x}) + \alpha \int_{\Omega} [g(\mathbf{x})]^T [g(\mathbf{x})]\, d\Omega \tag{9}$$

where the constraint $g(\mathbf{x}) = 0$ is imposed in the volume $\Omega$ in the limit as the positive penalty parameter $\alpha \to \infty$.

Several points can be made about the penalty formulation:

(1) Imposing the constraint in this manner is exactly the same as the standard variational procedure [9] of removing a boundary condition restriction on the trial function by adding a suitable integral to the functional, except that the added term is here positive semi-definite. In each case, the resulting Euler equations include the required constraint or boundary condition.

(2) The constraint is imposed in the least-squared sense.

(3) As will be shown in Section III, physical significance can be attached to $\alpha$.

(4) The larger the value of $\alpha$, the more heavily is the constraint imposed on the trial function.

In this paper the penalty function method will be used. To appreciate the power of the technique a brief digression to survey some of the applications of the method is justified. The penalty function method has its origins in operational research and was later adopted by scientists and engineers engaged on finite element analysis when a variational principle has to be supplemented by a constraint. For example Zienkiewicz [10] considers the problem of beam bending using $C^0$ trial functions, the required $C^1$ continuity being imposed by the penalty function method. Bercovier and Engelman [11] and Hughes, Liu and Brooks [12] both address the problem of viscous incompressible flow where the incompressibility is forced by the penalty function. Hamdi and Ousset [13] apply a penalty function to a coupled fluid-structure system.

In each of these examples the authors report success provided reduced integration is used. Reasons for the success of this technique are suggested by Zienkiewicz and Hinton [14]. They concentrate on equations of the form $\mathbf{Ax} = \mathbf{b}$ and show that in some situations reduced integration is vital to obtain correct answers. In this paper a time harmonic propagation problem is considered and it will be shown that reduced integration, although advantageous, is not vital.

Since the constraint is imposed in the limit as $\alpha \to \infty$, one might expect problems of numerical ill-conditioning. In practice, this problem did not occur, acceptable solutions being obtained well before ill-conditioning arose.

When the penalty term is incorporated into the system equations the eigenvalue problem can be written as

$$(\mathbf{K} + \alpha \mathbf{K}_1)\, \mathbf{x} = \lambda \mathbf{M} \mathbf{x} \tag{10}$$

where $\mathbf{K}$ is the system stiffness matrix due to the unconstrained functional, $\mathbf{K}_1$ is the contribution to the system stiffness matrix from the penalty function, $\lambda = \omega^2$ is the

eigenvalue, $\omega$ is the resonant frequency in radians/second and $\mathbf{M}$ is the system mass matrix. Clearly, as $\alpha \to \infty$, (10) approaches

$$\alpha \mathbf{K}_1 \mathbf{x} = \lambda \mathbf{M} \mathbf{x} \tag{11}$$

and as $\alpha$ increases, $\lambda$ increases. To limit this error increase in the eigenvalue a technique known as reduced integration [15] is used.

### C. *Reduced Integration*

It is known that the resonant frequencies computed numerically in the finite element method are upper bound approximations on the exact resonant frequencies of the system. This means that the system is too stiff. It is found [15] that by evaluating the element stiffness matrices with a reduced order of integration improved answers can be obtained, provided that the error in the numerical scheme systematically compensates for the upper bound approximation on the stiffness calculated by the finite element method. If, however, too low an integration scheme is used, then unsatisfactory results are obtained.

## III. Example

In this section an example of the penalty formulation applied to a finite element eigenvalue problem is considered. The problem chosen is that of finding the resonances of a contained cylinder of water subject to the boundary condition that the normal component of the velocity vanishes over the surface $S$ of the cylinder. One method of avoiding spurious modes would be to define the problem in terms of a scalar potential. We have avoided this approach because the work described in this paper is the first stage in the development of a computer program to model the propagation of elastic waves in an acoustic microscope [16]. This involves waves propagating through a liquid–solid interface, and so the particle velocity is a convenient choice of field variable throughout the volume. Thus we require the solution of

$$c_{11} \nabla [\nabla \cdot \mathbf{v}] = \rho (\partial^2 \mathbf{v} / \partial t^2) \tag{6}$$

subject to the boundary condition

$$\mathbf{v} \cdot \hat{\mathbf{n}} = 0 \tag{6a}$$

where $\hat{\mathbf{n}}$ is the unit normal vector, and to the constraint

$$\nabla \times \mathbf{v} = 0 \tag{6b}$$

everywhere in the cylinder.

It is assumed that the problem is axisymmetric, that is, there is no velocity component $v_\theta$ and the fields have no $\theta$ angular dependence. Under these conditions and assuming harmonic time dependence, (6) may be easily solved for $v_r$ and $v_z$;

$$v_r = AkJ_1(kr)\cos\beta z \tag{12}$$

$$v_z = A\beta J_0(kr)\sin\beta z \tag{13}$$

where $A$ is an arbitrary constant, $\beta$ is the phase constant, $J_0$ and $J_1$ are the usual Bessel functions and

$$(\omega/V_l)^2 = k^2 + \beta^2 \tag{14a}$$

$$V_l = (c_{11}/\rho)^{1/2}. \tag{14b}$$

Imposing the boundary condition $\mathbf{v}\cdot\hat{\mathbf{n}} = 0$ on (12) and (13) shows that

$$ka = p_m \tag{15}$$

and

$$\beta = n\pi/l \tag{16}$$

where $l$ and $a$ are the length and radius of the cylinder, respectively, and $p_m$ are the roots of $J_1(p) = 0$, i.e., $p_0 = 0$, $p_1 = 3.832$, $p_2 = 7.016$, etc. In the example considered $l = 0.40$ metres and $a = 0.15$ metres. Table I shows the first eight analytically calculated modes. The nomenclature used is $T_{mn}$, where $m$ and $n$ are defined by (15) and (16), respectively. From the table it is seen that there are five scalar modes (i.e., modes in which one of the two components is identically zero) and three vector modes.

TABLE I

The First Eight Analytically Calculated Modes for a Contained Cylinder of Water

| | | $\beta$ | $k$ | $\omega$ |
|---|---|---|---|---|
| 1 | $T_{01}$ | 7.8540 | 0 | 12174. |
| 2 | $T_{02}$ | 15.7080 | 0 | 24347. |
| 3 | $T_{03}$ | 23.5619 | 0 | 36251. |
| 4 | $T_{10}$ | 0 | 25.5447 | 39594. |
| 5 | $T_{11}$ | 7.8540 | 25.5447 | 41423. |
| 6 | $T_{12}$ | 15.7080 | 25.5447 | 46481. |
| 7 | $T_{04}$ | 31.4159 | 0 | 48695. |
| 8 | $T_{13}$ | 23.5619 | 25.5447 | 53866. |

*Note.* $\beta$ and $k$ are in rad/m, and $\omega$ is in rad/s, assuming a velocity of sound of 1550 m/s.

Auld [8] shows that

$$\omega^2 = \frac{\int_\Omega (\mathbf{Av})^T \mathbf{c}(\mathbf{Av})\, d\Omega - \int_S \mathbf{v}^T \cdot [\mathbf{cAv}] \cdot \mathbf{d\hat{s}}}{\int_\Omega \mathbf{v}^T \rho \mathbf{v}\, d\Omega} \tag{17}$$

is the starting point for deriving a number of different functionals. By considering a small perturbation about the exact solution it can be shown that (17) is indeed a functional corresponding to the Euler equation (6) provided $c_{44} = 0$ and the boundary condition $\mathbf{v} \cdot \hat{\mathbf{n}} = 0$ is forced on the trial function. In (17), $\mathbf{A}$ is the matrix relating strain and displacement, $\mathbf{c}$ is the stiffness matrix and $S$ is the surface of the volume $\Omega$. If we modify the functional (17) to include the penalty $\nabla \times \mathbf{v} = 0$, the new functional is

$$\omega^2 = \frac{\int_\Omega (\mathbf{Av})^T \mathbf{c}(\mathbf{Av})\, d\Omega - \int_S \mathbf{v}^T \cdot [\mathbf{cAv}] \cdot \mathbf{d\hat{s}} + \alpha \int_\Omega [\nabla \times \mathbf{v}]^T [\nabla \times \mathbf{v}]\, d\Omega}{\int_\Omega \mathbf{v}^T \rho \mathbf{v}\, d\Omega}. \tag{18}$$

It is easily shown that the Euler equation for (18) indeed includes $\nabla \times \mathbf{v} = 0$—the penalty that is being imposed. The penalty term is suppressing any rotational energy that could appear in the unconstrained functional (17). $\alpha$ has units of $N/m$ and represents the shear modulus of the liquid, which should be zero. We therefore have a conflict between the "physics of the problem," which states that $\alpha \to 0$ and the "mathematics of the problem," which states that $\alpha \to \infty$. Assuming that there exist both compression and shear wave components in the solution obtained with the unconstrained functional (17) (i.e., neither $\nabla \times \mathbf{v}$ nor $\nabla \cdot \mathbf{v}$ are identically zero), then for the same boundary conditions and forcing function, an increasingly large shear modulus ($\alpha \to \infty$) implies an ever smaller amplitude of any shear waves present. Thus the eigenvectors become more and more heavily weighted towards compression velocity modes only. Alternatively, any shear waves present can be eliminated by allowing the shear modulus to approach zero. Thus there is no discrepancy between the physical and mathematical arguments. They are just alternative ways of considering the same phenomenon.

## IV. Results

A computer program was written to solve the problem using finite elements. The mesh used is shown in Fig. 1 and consists of 24 triangular elements and 63 nodes with two degrees of freedom ($v_r$ and $v_z$) at each node. As is evident, quadratic basis functions are used. Double precision arithmetic (64 bits) was used in the program.

### A. *Imposing a Curl Free Constraint*

Figures 2 and 3 show how the $T_{11}$ and $T_{12}$ modes, respectively, move down the spectrum of eigenvalues as the penalty parameter increases. The $T_{11}$ and $T_{12}$ modes

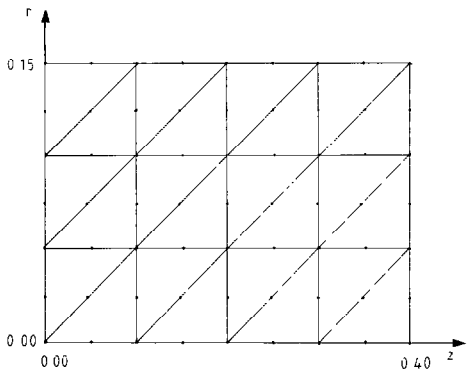


FIG. 1. A longitudinal section through the $r$–$z$ plane showing the mesh used.

lock into positions 5 and 6 in the spectrum, respectively. This is correct, as can be seen from Table I. The results presented in these two figures are obtained for both full (error $= O(h^4)$) and reduced (error $= O(h^3)$) integration of the penalty term. Figures 4 and 5 show the variation in the error in the frequency for these two modes as the penalty parameter increases. The results for both full and reduced integration are plotted on each figure and it can be seen that the use of reduced integration results in a smaller increase in error in the frequency. This is expected from the above theory.

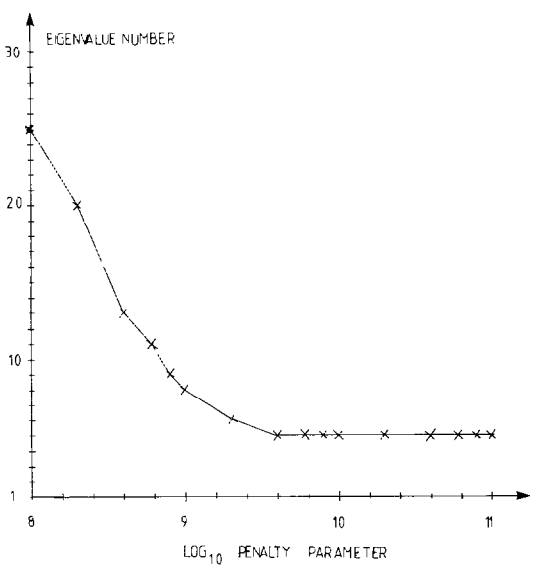


FIG. 2. A graph showing how the $T_{11}$ mode moves down the spectrum of eigenvalues as the penalty parameter increases.

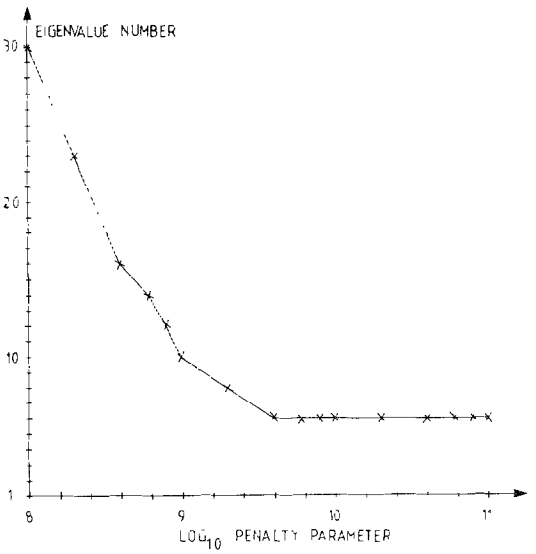


FIG. 3. A graph showing how the $T_{12}$ mode moves down the spectrum of eigenvalues as the penalty parameter increases.

Table II shows how the spectrum of eigenvalues, for the first eight physical modes only, varies as the penalty parameter increases. From the table it is seen that as the penalty parameter increases, an increasing number of spurious modes are eliminated and the physical modes gradually move to the bottom of the spectrum. When $\alpha = 6 \times 10^9\ N/m$, there are no spurious modes in the first eight eigenvalues. However,

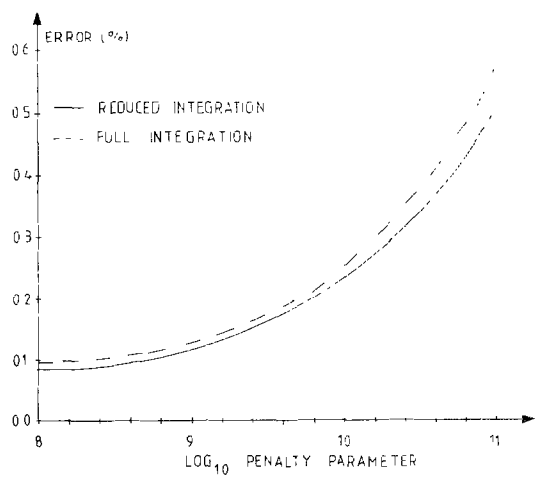


FIG. 4. The variation of the error in the resonant frequency for the mode $T_{11}$ with penalty parameter. The results for both full and reduced integration are plotted.

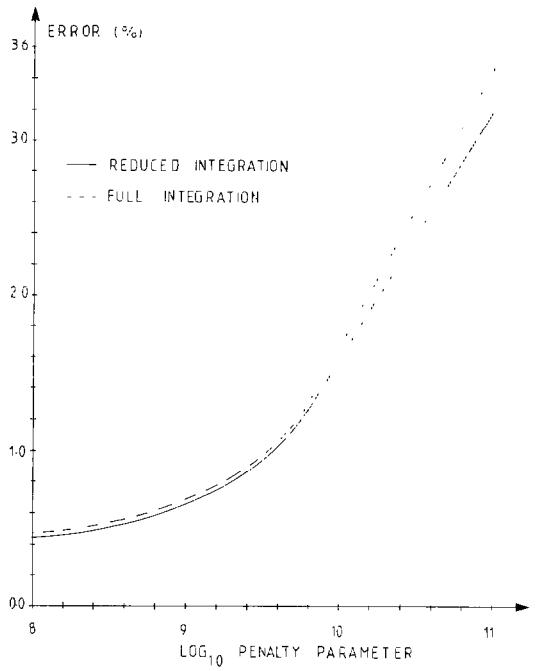


FIG. 5. The variation of the error in the resonant frequency for the mode $T_{12}$ with penalty parameter. The results for both full and reduced integration are plotted.

TABLE

The Variation of the Spectrum of

| Eigenvalue number | 1 | 2 | 3 | 4 | 5 | 6 | 7 | 8 | 9 | 10 | 11 | 12 | 13 | 14 | 15 | 16 | 17 |
|---|---|---|---|---|---|---|---|---|---|---|---|---|---|---|---|---|---|
| Penalty parameter 0 | S | S | S | S | S | S | S | S | S | S | S | S | S | S | S | S | S |
| $10^8$ | S | S | 01 | S | S | S | S | S | S | S | S | 02 | S | S | S | S | S |
| $2 \times 10^8$ | S | 01 | S | S | S | S | S | 02 | S | S | S | S | S | S | 03 | S | S |
| $4 \times 10^8$ | 01 | S | S | S | 02 | S | S | S | S | S | 03 | 10 | 11 | S | 12 | S | S |
| $6 \times 10^8$ | 01 | S | S | 02 | S | S | S | 03 | S | 10 | 11 | S | S | 12 | 04 | S | 13 |
| $8 \times 10^8$ | 01 | S | 02 | S | S | 03 | S | 10 | 11 | S | S | 12 | S | 04 | S | 13 | |
| $10^9$ | 01 | 02 | S | S | S | 03 | 10 | 11 | S | 12 | S | 04 | S | S | 13 | | |
| $2 \times 10^9$ | 01 | 02 | 03 | S | 10 | 11 | S | 12 | 04 | S | 13 | | | | | | |
| $4 \times 10^9$ | 01 | 02 | 03 | 10 | 11 | 12 | 04 | S | 13 | | | | | | | | |
| $6 \times 10^9$ | 01 | 02 | 03 | 10 | 11 | 12 | 04 | 13 | | | | | | | | | |

*Note.* The first and second digits for each physical mode are the values of $m$ and $n$, respectively, in the nomenclature $T_{mn}$. $S$ denotes a spurious mode.

there are spurious modes higher up the spectrum but their elimination is not possible because with the value of $\alpha$ used they have not yet been sufficiently constrained.

Figures 6a and 6b show the other major advantage to be gained by constraining the functional. They show for the $T_{01}$ mode the same physical field with no constraint ($\alpha = 0$), Fig. 6a, and with a value of $\alpha$ of $6 \times 10^9$ using reduced integration of the penalty, Fig. 6b. Only the non-zero component ($v_z$) is shown. The improvement in the quality of the eigenvector is evident. Whilst it is possible to discard, incorrectly in this case, the eigenvector in Fig. 6a as spurious, the same cannot be said for the eigenvector in Fig. 6b, although they both represent the same physical field (a scalar field). Furthermore, the approximation to zero for the other component, $v_r$, is substantially better with the penalty function than without it.

It was pointed out in Section II C that if too low an integration order is used when evaluating the penalty poor results may arise. This was confirmed numerically by integrating the penalty function using a scheme whose error is $O(h^2)$. Many spurious modes were obtained, even when a high penalty parameter value was used. The reason for this is that many terms in each element matrix derived from the penalty function are zero and so the constraint is only approximately imposed on the functional (17).

Silvester [17] points out that significantly improved results are obtained when high order basis functions are used. This is all the more true when a penalty is imposed because

(1) first order basis functions rule out reduced integration if the penalty term involves their derivatives and

(2) the higher the order of the basis function, the lower the increase in the error in the resonant frequency and so the more accurate the result.

II

Eigenvectors as the Penalty Parameter Increases

| 18 | 19 | 20 | 21 | 22 | 23 | 24 | 25 | 26 | 27 | 28 | 29 | 30 | 31 | 32 | 33 | 34 | 35 | 36 | 37 | 38 | 39 | 40 | 41 |
|---|---|---|---|---|---|---|---|---|---|---|---|---|---|---|---|---|---|---|---|---|---|---|---|
| S | S | S | S | S | S | 01 | S | 02 | S | S | S | S | S | S | 03 | S | 10 | 11 | S | 12 | 04 | S | 13 |
| S | S | S | 03 | S | S | 10 | 11 | S | S | S | S | 12 | 04 | S | S | S | S | 13 | | | | | |
| 10 | S | 11 | S | S | 12 | S | S | 04 | S | 13 | | | | | | | | | | | | | |
| S | 04 | S | S | 13 | | | | | | | | | | | | | | | | | | | |

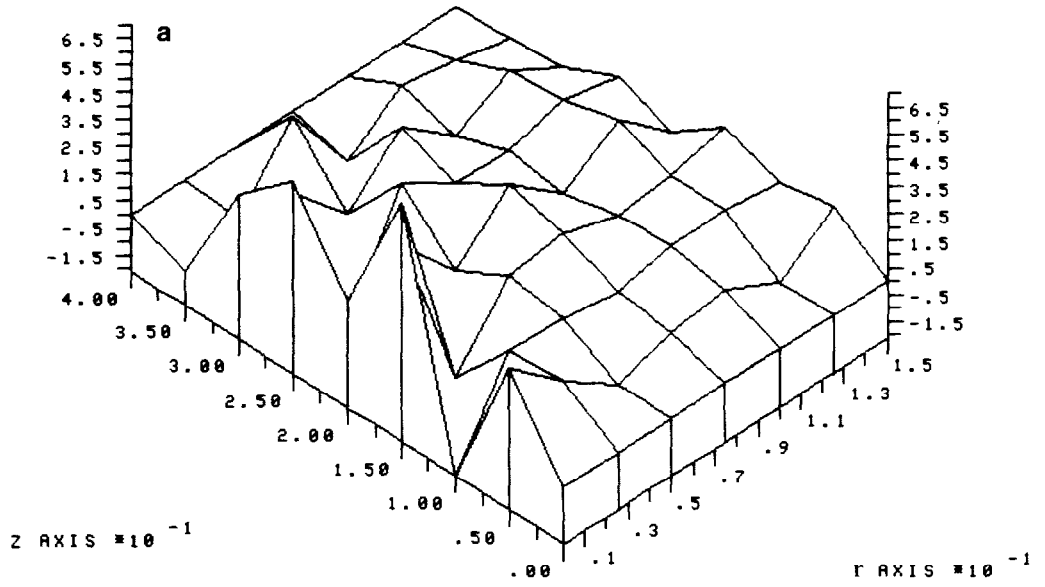


FIG. 6a. The mode $T_{01}$ obtained with no constraint aplied to the functional. Only the $v_z$ component is shown.

## B. *Further Tests*

In Section II A the analogy between electromagnetic wave propagation and acoustic wave propagation in liquids was presented and in Section IV A the results of the acoustic problem were presented. Rahman and Davies [19] have used the finite element method, using constrained and unconstrained functionals, to analyse optical waveguides. Specifically, they used the **H** field functional (2) and compare the results with and without the divergence free penalty. Their results are in agreement with those presented here, namely, the gradual removal of the spurious solutions from the bottom of the spectrum and a marked improvement in the quality of the eigenvector of the physical modes.

Finally, it is interesting to note that with the unconstrained functional (17) the first three eigenvalues are all of the order of $10^{-3}$, but the fourth eigenvalue is of the order of $10^5$ and thereafter there is a smooth increase in the value of the eigenvalues. The large increase in magnitude between the third and fourth eigenvalues suggests that the near-zero eigenvalues are due to instability in the equations. When the curl free constraint is imposed, the first three eigenvalues disappear, suggesting that the

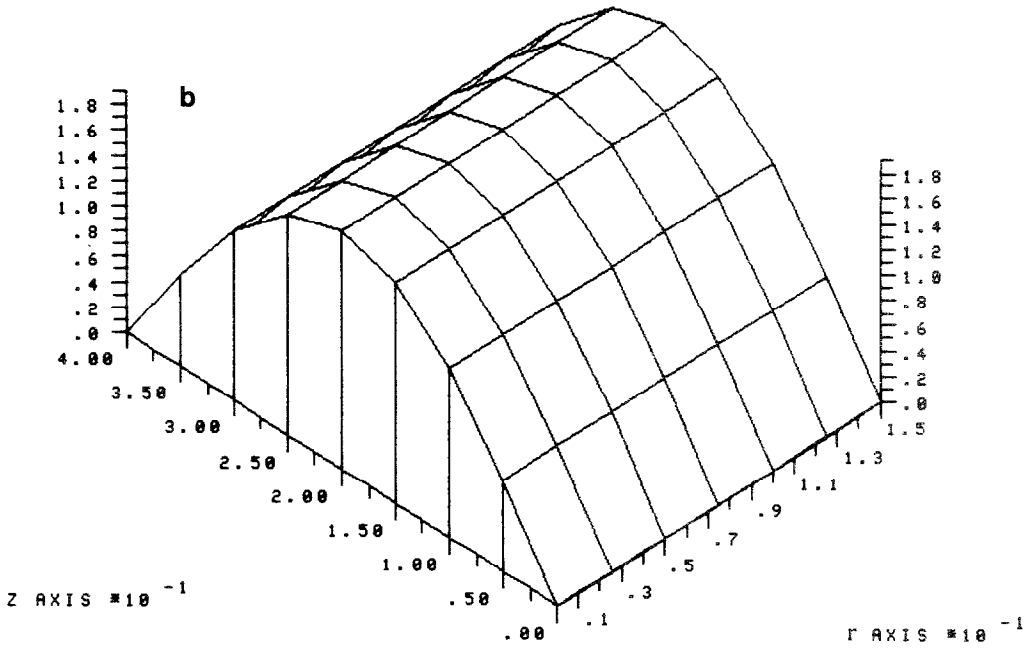


FIG. 6b. The mode $T_{01}$ obtained by minimising the constrained functional. Reduced integration is used. Only the $v_z$ component is shown.

constraint confers stability on the equations. Kiefling and Feng [6] similarly report a cluster of near-zero frequency spurious modes and study the effect of varying the mesh size.

## V. CONCLUSIONS

A study of spurious modes that arise in eigenvalue problems has been carried out. It has been shown that a major cause of these spurious modes is ambiguity in the problem statement. Three methods were considered for removing the ambiguity but two were rejected for computational reasons. The third method, the penalty method was used and proved to be very successful. This is a limiting process in which the penalty is forced on the solution as the penalty parameter tends to infinity. This means that only among the lower order physical modes can the spurious modes be eliminated but this is not serious because we are normally only interested in these lower order modes.

Reduced integration was used to limit the increase in error in the frequency that occurs when a constrained functional is minimised. It was shown that care needs to be taken in choosing the correct integration order. As well as eliminating spurious modes, constraining the functional substantially improves the quality of the eigenvector of the physical modes.

The analogy between electromagnetic wave propagation and elastic waves in compressible liquids was emphasized. Both theoretical and computational evidence were presented to show that in their vector solution by the finite element method and in the occurrence or avoidance of non-physical solutions, the two wave types have many properties in common.

## REFERENCES

1. A. J. DAVIES, "The Finite Element Method," Oxford Univ. Press (Clarendon), Oxford, 1980.
2. A. KONRAD, *IEEE Trans. Microwave Theory Tech.* **MTT-24** (1976), 553–559.
3. J. B. DAVIES, F. A. FERNANDEZ, AND G. Y. PHILIPPOU, *IEEE Trans. Microwave Theory Tech.* **MTT-30** (1982), 1975–1980.
4. M. IKEUCHI, K. INOUE, H. SAWAMI, AND H. NIKI, *Trans. Inst. Elec. Engrg. Japan A* **98** (1978), 415–422.
5. N. MABAYA, P. E. LAGASSE, AND P. VANDENBULCKE, *IEEE Trans. Microwave Theory Tech.* **MTT-29** (1981), 600–605.
6. L. KIEFLING AND G. C. FENG, *AIAA J.* **14**, No. 2 (1976), 199–203.
7. B. A. AULD, "Acoustic Fields and Waves in Solids," Vol. 1, Chap. 6, Wiley, New York, 1973.
8. B. A. AULD, "Acoustic Fields and Waves in Solids," Vol. 2, Chap. 13, Wiley, New York, 1973.
9. P. M. MORSE AND H. FESHBACH, "Methods of Theoretical Physics," Part 2, pp. 1131–1133, McGraw–Hill, New York, 1953.
10. O. C. ZIENKIEWICZ, "The Finite Element Method," 3rd ed., Chap. 11, McGraw–Hill, New York, 1977.
11. M. BERCOVIER AND M. ENGELMAN, *J. Comput. Phys.* **30** (1979), 181–201.
12. T. J. R. HUGHES, W. K. LIU, AND A. BROOKS, *J. Comput. Phys.* **30** (1979), 1–60.
13. M. A. HAMDI, AND Y. OUSSET, *Internat. J. Numer. Methods Engrg.* **13** (1978), 139–150.
14. O. C. ZIENKIEWICZ AND E. HINTON, *J. Franklin Inst.* **302**, Nos. 5 and 6 (1976), 443–461.
15. K. J. BATHE, "Finite Element Procedures in Engineering Analysis," Prentice–Hall, Englewood Cliffs, N.J., 1982.
16. C. F. QUATE, A. ATALAR, AND H. K. WICKRAMASINGHE, *Proc. IEEE* **67**, No. 8 (1979), 1092–1113.
17. P. SILVESTER, *Internat. J. Engrg. Sci.* **7** (1969), 849–861.
18. A. D. BERK, *IRE Trans. Antennas and Propagation* **AP-4** (1956), 104–111.
19. B. M. A. RAHMAN AND J. B. DAVIES, *IEEE Trans. Microwave Theory Tech.* **MTT-30** (1984).